

In contrast, no conformational changes of rHSA were observed upon mutating Cys in position 34 to a serine.

### Functional Properties

The high-affinity binding of warfarin and ketoprofen was studied to examine whether the exceptional drug binding properties of HSA had been affected by the mutation and the oxidations. In both examples, only CT<sub>10</sub>-HSA and CT<sub>50</sub>-HSA showed reduced drug binding properties. The decreased binding of warfarin to CT<sub>10</sub>-HSA can be explained by conformational changes taking place in subdomain IIA and the oxidation of one or more of the Met residues at positions 298, 329 or 446. In CT<sub>50</sub>-HSA these explanations could be supplemented with oxidation of relevant lysine or arginine residues. However, in both cases, the oxidation of <sup>214</sup>Trp could contribute to the diminished binding, because a previous study has shown that mutation of <sup>214</sup>Trp to an alanine results in decreased warfarin binding (25). The decreased ketoprofen binding to CT<sub>10</sub>-HSA and CT<sub>50</sub>-HSA is most likely the result of conformational changes involving site II in subdomain IIIA (7). The decreased binding to the latter protein can also be caused by oxidation of <sup>410</sup>Arg.

The esterase-like activity of HSA is caused by the proximity of <sup>410</sup>Arg and <sup>411</sup>Tyr in subdomain IIIA (17). This function is only impaired in the case of CT<sub>10</sub>-HSA and CT<sub>50</sub>-HSA. The finding is probably the result of conformational changes that affect the orientation of the two residues. In the latter case, however, <sup>410</sup>Arg could have been oxidized as well.

### Pharmacokinetics

Neither the mutation of <sup>34</sup>Cys for a serine nor the relatively extensive oxidation of HSA (CT<sub>10</sub>-HSA) had any effect on its plasma half-life or liver clearance in mice (Table III). However, CT<sub>50</sub>-HSA was modified to such a degree that its plasma half-life was decreased to a considerable extent from ca. 20 min to ca. 9 min. This finding can be explained by a ca. 11-fold increase in liver uptake clearance. The increased liver clearance is probably due to an increased endocytosis of the protein by scavenger receptors of endothelial, Kupffer cells (26). In contrast to liver clearance, the uptake by heart, lung, spleen, and kidney were in all cases unaffected by the protein modifications. The authors have not estimated the clearance of other tissues or organs. However, in the future detailed examinations of this will be carried out using cell lines.

### CONCLUSION

As illustrated by the column experiments with serum, the authors succeeded in constructing an oxidation model using HSA. Functional studies, performed *in vitro*, with the different albumin preparations indicate that Site II is more effected than Site I and <sup>34</sup>Cys in HSA, when it is exposed to oxidative stress.

### REFERENCES

1. I. Climent, L. Tsai, and R. L. Levine. Derivatization of  $\gamma$ -glutamyl semialdehyde residues in oxidized proteins by fluorescein-amine. *Anal. Biochem.* **182**:226–232 (1989).
2. E. Bourdon, N. Loreau, and D. Blache. Glucose and free radicals impair the antioxidant properties of serum albumin. *FASEB J.* **13**:233–244 (1999).
3. S. Sugio, A. Kashima, S. Mochizuki, M. Noda, and K. Kobayashi. Crystal structure of human serum albumin at 2.5 Å resolution. *Protein Eng.* **12**:439–446 (1999).
4. M. Anraku, K. Yamasaki, T. Maruyama, U. Kragh-Hansen, and M. Otagiri. Effect of oxidative stress on the structure and function of human serum albumin. *Pharm. Res.* **18**:632–639 (2001).
5. S. Era, T. Hamaguchi, M. Sogami, K. Kuwata, E. Suzuki, K. Miura, K. Kawai, Y. Kitazawa, H. Okabe, A. Noma, and S. Miyata. Further studies on the resolution of human mercapt- and non-mercaptalbumin and on human serum albumin in the elderly by high-performance liquid chromatography. *Int. J. Pept. Protein Res.* **31**:435–442 (1988).
6. M. Sogami, S. Nagaoka, S. Era, M. Honda, and K. Noguchi. Resolution of human mercapt and nonmercaptalbumin by high performance liquid chromatography. *Int. J. Pept. Protein Res.* **24**:96–103 (1984).
7. M. Sogami, S. Era, S. Nagaoka, K. Kuwata, K. Kida, K. Miura, H. Inouye, E. Suzuki, S. Hayano, and S. Sawada. HPLC-studies on nonmercapt-mercapt conversion of human serum albumin. *Int. J. Pept. Protein Res.* **24**:398–402 (1985).
8. Y. Shechter, Y. Burstein, and A. Patchornik. Selective oxidation of methionine residues in proteins. *Biochemistry* **14**:4497–4503 (1975).
9. R. F. Chen. Removal of fatty acids from serum albumin by charcoal treatment. *J. Biol. Chem.* **242**:173–181 (1967).
10. S. Era, K. Kuwata, H. Imai, K. Nakamura, T. Hayashi, and M. Sogami. Age-related change in redox state of human serum albumin. *Biochim. Biophys. Acta* **1247**:12–16 (1995).
11. H. Watanabe, K. Yamasaki, U. Kragh-Hansen, S. Tanase, K. Harada, A. Suenaga, and M. Otagiri. *In vitro* and *in vivo* properties of recombinant human serum albumin from *Pichia pastoris* purified by a method of short processing time. *Pharm. Res.* **18**:1775–1781 (2001).
12. T. Hayashi, S. Era, K. Kawai, H. Imai, K. Nakamura, E. Onda, and M. Yoh. Observation for redox state of human serum and aqueous humor albumin from patients with senile cataract. *Pathophysiology* **6**:237–243 (2000).
13. K. Takabayashi, T. Imada, Y. Saito, and Y. Inada. Coupling between fatty acid binding and sulfhydryl oxidation in bovine serum albumin. *Eur. J. Biochem.* **136**:291–295 (1983).
14. T. Zor and Z. Selinger. Linearization of the Bradford protein assay increases its sensitivity: theoretical and experimental studies. *Anal. Biochem.* **236**:302–308 (1996).
15. P. G. Pande, R. V. Nellore, and H. R. Bhagat. Optimization and validation of analytical conditions for bovine serum albumin using capillary electrophoresis. *Anal. Biochem.* **204**:103–106 (1992).
16. P. M. Horowitz, S. Hua, and D. L. Gibbons. Hydrophobic surfaces that are hidden in chaperonin Cpn60 can be exposed by formation of assembly-competent monomers or by ionic perturbation of the oligomer. *J. Biol. Chem.* **270**:1535–1542 (1995).
17. H. Watanabe, S. Tanase, K. Nakajou, T. Maruyama, U. Kragh-Hansen, and M. Otagiri. Role of Arg-410 and Tyr-411 in human serum albumin for ligand binding and esterase-like activity. *Biochem. J.* **349**:813–819 (2000).
18. Y. Takakura, T. Fujita, M. Hashida, and H. Sezaki. Disposition characteristics of macromolecules in tumor-bearing mice. *Pharm. Res.* **7**:339–346 (1990).
19. J. R. Duncan and M. J. Welch. Intracellular metabolism of indium-111-DTPA-labeled receptor targeted proteins. *J. Nucl. Med.* **34**:1728–1738 (1993).
20. K. Yamaoka, Y. Tanigawara, T. Nakagawa, and T. Uno. Pharmacokinetic analysis program (multi) for microcomputer. *J. Pharmacobiodyn.* **4**:879–885 (1981).
21. T. Mukai, Y. Arano, K. Nishida, H. Sasaki, H. Saji, and J. Nakamura. *In-vivo* evaluation of indium-111-diethylenetriaminepentaacetic acid-labelling for determining the sites and rates of protein catabolism in mice. *J. Pharm. Pharmacol.* **51**:15–20 (1999).
22. G. Sudlow, D. J. Birkett, and D. N. Wade. The characterization of two specific drug binding sites on human serum albumin. *Mol. Pharmacol.* **11**:824–832 (1975).

23. T. Peters, Jr. *All about Albumin: Biochemistry, Genetics, and Medical Applications*, Academic Press, San Diego, California, 1996.
24. V. T. G. Chuang, A. Kuniyasu, H. Nakayama, Y. Matsushita, S. Hirono, and M. Otagiri. Helix 6 of subdomain IIIA of human serum albumin is the region primarily photolabeled by ketoprofen, an arylpropionic acid NSAID containing a benzophenone moiety. *Biochim. Biophys. Acta* **1434**:18–30 (1999).
25. H. Watanabe, U. Kragh-Hansen, S. Tanase, K. Nakajou, M. Mitarai, Y. Iwao, T. Maruyama, and M. Otagiri. Conformational stability and warfarin-binding properties of human serum albumin studied by recombinant mutants. *Biochem. J.* **357**:269–274 (2001).
26. B. Smedsrod, J. Melkko, N. Araki, H. Sano, and S. Horiuchi. Advanced glycation end products are eliminated by scavenger-receptor-mediated endocytosis in hepatic sinusoidal, Kupffer and endothelial cells. *Biochem. J.* **322**:567–573 (1997).

## Probenecid-Induced Changes in the Clearance of Pranoprofen Enantiomers

TERUKO IMAI, TADAYUKI NOMURA, AND MASAKI OTAGIRI\*  
*Faculty of Pharmaceutical Sciences, Kumamoto University, Kumamoto, Japan*

**ABSTRACT** Probenecid is known to inhibit the elimination of several acidic drugs. Its influence on the pharmacokinetics of pranoprofen was investigated in rabbit after a single intravenous injection of racemic mixture (5 mg/kg). Levels of (–)-(R)- and (+)-(S)-pranoprofen and their glucuronide (after hydrolysis with sodium hydroxide) were determined in plasma, urine, and several tissues. The plasma concentration of the (+)-(S)-isomer was higher than that of the (–)-(R)-form. Oral coadministered probenecid (100 mg/kg) resulted in an increased plasma concentration of both enantiomers. Probenecid reduced the apparent total clearance and excretion of pranoprofen enantiomers in urine. It had a slight effect on the tissue distribution of pranoprofen at the dose used, but significantly reduced the formation of glucuronide for both enantiomers to the same extent in kidney microsomes. The differences caused by probenecid were significant with respect to its ability to inhibit glucuronidation in the kidney and subsequent excretion into urine, but enantioselective effects were negligible. *Chirality* 15:318–323, 2003. © 2003 Wiley-Liss, Inc.

**KEY WORDS:** enantioselective disposition; plasma concentration; glucuronidation; drug interaction; chiral inversion

Probenecid (*p*-(dipropylsulfamoyl)-benzoic acid), a non-chiral uricosuric agent, inhibits organic anion transport in the kidney and has been used clinically to inhibit the renal secretion of penicillin and cephalosporin antibiotics.<sup>1,2</sup> In vivo studies suggest that probenecid also inhibits the glucuronide conjugation of coadministered drugs through competition for uridine diphosphate glucuronyltransferase.<sup>3</sup> Probenecid and several substrates that contain hydroxy or carboxyl groups undergo glucuronidation prior to elimination. Conjugation increases the polarity of the substrate and confers a negative charge on the molecule, thereby facilitating the removal of xenobiotics from the body. The primary metabolic pathway for probenecid involves oxidation of the *N*-propyl sidechains, with subsequent conjugation to glucuronide.<sup>4</sup> Clinical studies suggest that probenecid may impair the glucuronidation of several drugs, including zomepirac,<sup>5</sup> carprofen,<sup>6</sup> ketoprofen,<sup>7</sup> zidovudine,<sup>8–10</sup> acetaminophen,<sup>11,12</sup> and lorazepam.<sup>11</sup>

Pranoprofen (2-5H-[1]benzopyrano[2,3-*b*]pyridine-7yl)propionic acid), a nonsteroidal antiinflammatory drug (NSAID), is biotransformed primarily by glucuronidation.<sup>13</sup> Significant differences in in vitro glucuronidation were found for pranoprofen enantiomers. In a previous study, we reported that the apparent  $V_{max}$  value for the glucuronidation of the (–)-(R)-enantiomer is 5.7-fold greater than that for the (+)-(S)-form in rabbit kidney microsomes, in spite of nearly the same  $K_m$  value between (–)-(R)- and (+)-(S)-enantiomers.<sup>13</sup> Differences in protein binding for the two enantiomers led to a 1.3–2.0-fold higher free fraction of (–)-(R)-pranoprofen. Therefore, the (–)-(R)-

isomer was found to be predominantly conjugated as an acyl glucuronide, and thus was excreted from the kidney rapidly in this form. Consequently, (+)-(S)-pranoprofen was present at a higher plasma concentration than the antipode in the rabbit. Furthermore, the (–)-(R)- and (+)-(S)-isoforms interact with each other in the elimination process through their conversion to the acyl glucuronide, resulting in different plasma concentration profiles for the racemate vis-à-vis the individual enantiomers.

It would be of interest to determine whether probenecid affects the disposition of pranoprofen, since it is well known that it alters the renal excretion of acidic compounds. Probenecid may competitively inhibit the formation of the glucuronide or may block the renal excretion of the conjugate, with subsequent chemical or enzymatic hydrolysis of the labile conjugate in vivo. Interactions of probenecid with NSAIDs such as carprofen,<sup>6</sup> ketoprofen,<sup>14</sup> and benoxaprofen<sup>15</sup> have previously been reported. Probenecid inhibits the elimination of NSAID through inhibition of acyl glucuronidation and the renal excretion of the glucuronide. Furthermore, in the case of ketoprofen and benoxaprofen, the enantiomeric ratio was significantly altered by probenecid, possibly because of an enhanced uni-

This paper was presented at the Symposium on Molecular Chirality 2003 in Kumamoto, Japan.

\*Correspondence to: Prof. Masaki Otagiri, Faculty of Pharmaceutical Sciences, Kumamoto University, 5-1 Oe-honmachi, Kumamoto 862-0973, Japan. E-mail: otagirim@gpo.kumamoto-u.ac.jp

Received for publication 30 August 2002; Accepted 1 November 2002  
 Published online 7 March 2003 in Wiley InterScience  
 (www.interscience.wiley.com). DOI: 10.1002/chir.10208

directional chiral inversion due to the reduced drug clearance. Because pranoprofen does not show chiral inversion in rabbits, it would be of interest to determine whether probenecid enantioselectivity affects the disposition of pranoprofen. The purpose of the present study was to determine the enantioselectivity of pharmacokinetic interactions of pranoprofen with probenecid in rabbits.

## EXPERIMENTAL

### Materials

Racemic pranoprofen and its enantiomers were a generous gift from Mitsubishi Welfide Co. (Tokyo, Japan). The optical purity of the (+)-(S)- and (-)-(R)-isomers were 98.4 and 97.9%, respectively. Uridine 5'-diphosphoglucuronic acid trisodium salt was purchased from Nacalai Tesque (Kyoto, Japan). All other chemicals and solvents were analytical grade.

### Animals

Male Japanese white rabbits (2.5–3.2 kg) were used. Rabbits were fasted for 24 h before the experiments, but water was available ad libitum. Racemic pranoprofen (5 mg/kg for the racemate), dissolved in 0.15 M phosphate buffer (pH 7.4), was injected into the ear vein. In the case of the coadministration of probenecid, probenecid (100 mg/kg) was orally administered into the stomach via a catheter 90 min before an injection of racemic pranoprofen. At appropriate intervals blood was withdrawn into a heparinized syringe from the ear vein. The plasma samples were adjusted to pH 3.5 by citrate buffer to prevent hydrolysis of glucuronide. A urine sample was obtained directly from the bladder using a ureter catheter and was collected in a pH 3.0 citrate buffer to prevent hydrolysis of glucuronide.

### Sample Treatment and Assay

(+)-(S)- and (-)-(R)-pranoprofen in plasma were determined by a previously described HPLC method.<sup>13</sup> One-half ml of 1 M HCl was added to the plasma sample (1 ml) and the pranoprofen was extracted with 6 ml of ether. The total concentration of pranoprofen was determined from 0.5 ml of plasma after hydrolysis of the glucuronide by the addition of 0.5 ml of 1 M NaOH for 1 h. The sample was then acidified with 0.5 ml of 2 M HCl and extracted with 6 ml of ether. In the case of urine, extraction was accomplished using benzene before and after hydrolysis of the glucuronide by treatment with base. The residue, obtained by evaporation of the organic phase, was dissolved in the HPLC mobile phase and injected into the HPLC. Methyl *p*-aminobenzoate was used as an internal standard. The HPLC assay was performed on a Chiralcel OJ column (25 × 2.6 mm i.d., Dical Chemical Industries, Tokyo, Japan) with a mobile phase comprised of *n*-heptan:2-propanol:acetic acid (70:40:1) at a flow rate of 1.0 ml/min using a Hitachi 655A-11 pump equipped with a Hitachi D-2500 chromatointegrator (Tokyo, Japan). Detection was at an excitation wavelength of 250 nm and an emission at 330 nm.

Probenecid in plasma (1 ml) was determined by the HPLC method after extraction from acidified plasma (1 M

HCl) with ether (6 ml). The HPLC assay was performed on LiChrosorb RP-18 column and detected at 248 nm.

### Tissue Distribution

In order to accurately measure the tissue concentration of pranoprofen, several tissues were collected at 45 min after an i.v. bolus injection of racemic pranoprofen (5 mg/kg). Each tissue was then homogenized in a 5 volume of phosphate-balanced solution (PBS). A 1 ml aliquot of the homogenate was then transferred to another test tube. The sum of pranoprofen and its glucuronide was determined after hydrolysis of the glucuronide by the addition of 0.5 ml of 1 M NaOH for 1 h. The sample was then acidified with 0.5 ml of 2 M HCl and extracted with benzene. The total concentration of pranoprofen enantiomers was determined by the HPLC method, as described above.

### Determination of Plasma Protein Binding

The free fraction of pranoprofen in plasma was measured by ultrafiltration using a micropartition system MPS-1 (Amicon Co., Danvers, MA) fitted with a membrane filter with a molecular weight cutoff value of 30,000. The plasma sample, containing 50 µg/ml of pranoprofen and 0–300 µg/ml of probenecid was applied to the reservoir and centrifuged at 2,000g for 10 min at 37°C. After centrifugation the filtrate was analyzed by HPLC. Since it has been reported that the plasma protein binding of pranoprofen in rabbit is maintained within a concentration range of 10–100 µg/ml,<sup>13</sup> the experiment was performed at 50 µg/ml of pranoprofen.

### Glucuronidation of Pranoprofen in Kidney Microsomes

Rabbits were exsanguinated from the carotid artery and the kidneys were removed immediately and homogenized in a Potter-Elvehjem homogenizer with 0.1 M Tris-HCl buffer (pH 7.4). The homogenate was centrifuged at 9,000g for 20 min and the resulting supernatant fluid was centrifuged 100,000g for 60 min to obtain microsomal pellets. The microsomal pellets were then resuspended in 0.1 M Tris-HCl buffer (pH 7.4). All procedures were done at 0–4°C. The incubation medium contained racemic pranoprofen, 2 mM uridine 5'-diphosphoglucuronic acid, 5 mM MgCl<sub>2</sub>, microsomes (2 mg as protein), 0.05% w/v Triton X-100, and 0.1 M Tris-HCl buffer at pH 7.4 in final volume of 2.0 ml. The incubation was carried out at 37°C for 30 min and terminated by adding 0.5 ml of 1 M HCl. The pranoprofen glucuronide was determined by a nonchiral analytical HPLC method using an LiChrosorb RP-18 column as described previously.<sup>13</sup>

## RESULTS AND DISCUSSION

### Plasma Concentration of Pranoprofen and Urinary Excretion of Its Glucuronide With and Without the Coadministration of Probenecid

Figure 1 shows the plasma concentration of probenecid after the oral administration of a 100 mg/kg dose. The highest concentration (24.8 ± 4.2 µg/ml, 88 ± 14.8 µM) of probenecid was detected at 1 h after dosing. The plasma concentration of probenecid then slowly decreased and a relatively high plasma concentration (9.2 ± 1.5 µg/ml) was

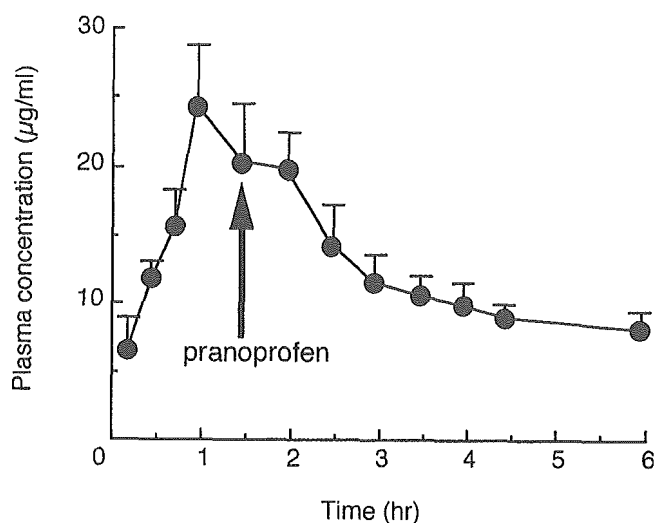


Fig. 1. Plasma concentration of probenecid after an oral administration of probenecid in rabbits. Values represent the mean  $\pm$  SD ( $n = 3$ ).

found even at 6 h after dosing. The elimination half-life of pranoprofen after an i.v. injection was previously reported to be 20 min in rabbits.<sup>13</sup> Therefore, pranoprofen (5 mg/kg) was injected at 90 min after the oral administration of probenecid (100 mg/kg).

Figure 2 shows the plasma concentration profile of pranoprofen with and without the administration of probenecid. The elimination of both (-)-(R)- and (+)-(S)-pranoprofen was inhibited by the coadministration of probenecid. The enantiomeric ratio (S/R ratio) of plasma concentration at each sampling point was not affected by probenecid, although the plasma concentration of pranoprofen was elevated by the coadministration of probenecid. These data clearly show that probenecid has no influence on the pattern of stereoselectivity in the pharmacokinetics of pranoprofen. The pharmacokinetic parameters calculated from plasma concentration using a two-compartment model are listed in Table 1. The coadministration of probenecid significantly reduced the rate constant ( $k_e$ ) and total clearance ( $CL_{tot}$ ) for the elimination of both pranoprofen isomers. However, the distribution volume ( $V_c$ ) remained unchanged. These findings are in agreement with data reported for 2-arylpropionic acid by several investigators.<sup>6,7,16</sup> Furthermore, Upton et al.<sup>7</sup> and Spahn et al.<sup>6</sup> reported a significant increase in the plasma concentration of the conjugated form of ketoprofen and carprofen, respectively, in spite of the fact that the clearance for their glucuronide formation decreased when probenecid was coadministered. They proposed that probenecid inhibits glucuronide formation of ketoprofen and carprofen and the subsequent renal elimination resulted in high plasma concentrations of both the parent acid and the corresponding glucuronide. We previously demonstrated that pranoprofen is conjugated to a glucuronide in the rabbit kidney and is sequentially excreted from the kidney because of the stability of the glucuronide in the kidney, compared with its remarkable instability in the liver.<sup>13</sup> Therefore, pranoprofen glucuronide could not be detected in plasma. In order to further investigate differences in the amount of

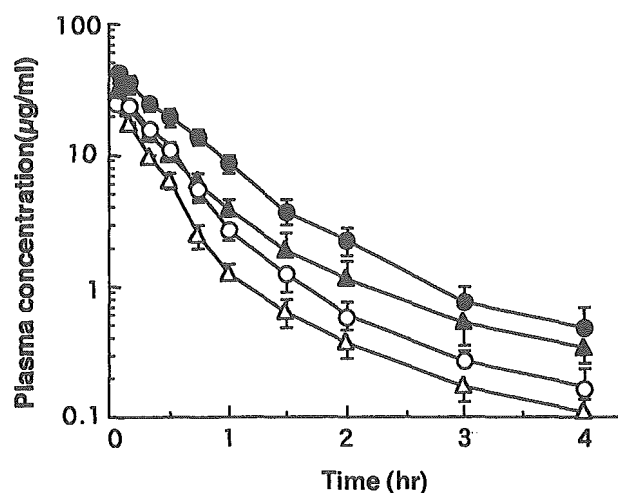


Fig. 2. Effect of orally administered probenecid on plasma concentration of (+)-(S)- and (-)-(R)-pranoprofen after an i.v. bolus injection of racemic pranoprofen in rabbits. Values represent the mean  $\pm$  SD ( $n = 3$ ). (+)-(S)-pranoprofen:  $\circ$ , without probenecid;  $\bullet$ , with probenecid. (-)-(R)-pranoprofen:  $\triangle$ , without probenecid;  $\blacktriangle$ , with probenecid. Dose: 5 mg/kg of pranoprofen and 100 mg/kg of probenecid.

pranoprofen converted to the glucuronide in the presence and absence of probenecid, the concentration of pranoprofen conjugate in the urine was determined. Probenecid was detected in the urine only after hydrolysis, indicating that only pranoprofen glucuronide was excreted in the urine, regardless of the coadministration of probenecid. As shown in Figure 3, the urinary excretion of pranoprofen glucuronide was retarded in the presence of probenecid. However, the S/R ratio of urinary excreted glucuronide was not affected by probenecid. These observations suggest that the elimination of (-)-(R)- and (+)-(S)-pranoprofen are inhibited by probenecid to the same extent.

#### Effect of Probenecid on Tissue Distribution of Pranoprofen

Some 2-aryl propionic acid is displaced from plasma proteins by probenecid.<sup>7,17</sup> For example, the fractions of free (+)-(S)- and (-)-(R)-carprofen in human plasma was increased by 79% and 44%, respectively, in the presence of probenecid.<sup>6</sup> Plasma protein binding is an important factor in tissue distribution because only a free drug can be transferred to tissue. The plasma protein binding of pranoprofen was then estimated with and without the coadministration of probenecid. The percentage of protein bound pranoprofen in plasma decreased in the presence of high concentrations of probenecid, as shown in Table 2, but the enantiomeric ratio remained unchanged. However, the free fraction of (+)-(S)- and (-)-(R)-pranoprofen in plasma was increased by 66% and 35% with the addition of 300  $\mu$ g/ml of probenecid, respectively. From the increasing free fraction of pranoprofen, increases in the tissue distribution and the clearance of pranoprofen would be expected.

The concentration of pranoprofen in several tissues at 45 min after an i.v. bolus injection of pranoprofen is shown in Table 3. In the administration of pranoprofen without probenecid, the normalized values obtained by dividing the

**TABLE 1. Pharmacokinetic parameters of (+)-(S)- and (-)-(R)-pranopfen after i.v. bolus administration of racemate with or without coadministration of probenecid**

|                           | Without probenecid |                           | With probenecid          |                            |
|---------------------------|--------------------|---------------------------|--------------------------|----------------------------|
|                           | (-)-(R)-pranopfen  | (+)-(S)-pranopfen         | (-)-(R)-pranopfen        | (+)-(S)-pranopfen          |
| ke (hr <sup>-1</sup> )    | 3.30 ± 0.48        | 2.62 ± 0.44 <sup>b</sup>  | 2.63 ± 0.18 <sup>a</sup> | 1.94 ± 0.15 <sup>a,b</sup> |
| Vc (ml)                   | 185 ± 9.21         | 150 ± 8.81 <sup>b</sup>   | 184 ± 33.8               | 145 ± 28.9 <sup>b</sup>    |
| AUC (µg/ml · hr)          | 11.12 ± 1.34       | 17.48 ± 2.40 <sup>b</sup> | 16.4 ± 2.06 <sup>a</sup> | 29.0 ± 4.79 <sup>a,b</sup> |
| CL <sub>tot</sub> (ml/hr) | 601 ± 60.1         | 386 ± 45.6 <sup>b</sup>   | 473 ± 53.0 <sup>a</sup>  | 275 ± 46.9 <sup>a,b</sup>  |

<sup>a</sup>P < 0.05 vs. the absence of probenecid.

<sup>b</sup>P < 0.05 vs. (-)-(R)-form.

tissue pranopfen by plasma concentration were greater for the (-)-(R)-isomer than for the (+)-(S)-isomer. The results are in good agreement with the free fraction of pranopfen in plasma. Especially, the concentration of (-)-(R)- and (+)-(S)-pranopfen and their ratio were highest in the kidney, where (-)-(R)-pranopfen was preferentially metabolized to conjugate<sup>13</sup> because both pranopfen and its conjugate were measured together. However, probenecid had only a slight effect on the tissue distribution of pranopfen, although the free fraction of pranopfen increased when probenecid was coadministered. Furthermore, the elimination clearance of pranopfen did not increase in the presence of probenecid (Table 1). Therefore, it appears that the increased free fraction of pranopfen in plasma has little effect on the disposition of pranopfen, possibly due to insufficient inhibition of pranopfen by low plasma concentrations of probenecid.

It has been reported that the transport of organic anions in several tissues is mediated by specific transporters and probenecid has been reported to be a particularly effective substrate and inhibitor of organic anion transporters.<sup>18,19</sup> NSAID drugs are also good substrates for organic transporters and accumulate in the kidney.<sup>20</sup> Furthermore, NSAIDs such as salicylic acid and indomethacin accumu-

late in the proximal tubules in the kidney and this accumulation is significantly decreased by the presence of probenecid.<sup>21</sup> It has also been reported that probenecid competitively inhibits the renal tubular secretion of a number of weak organic acids including NSAID and the tubular reabsorption of uric acid.<sup>2</sup> Therefore, it is possible that tissue distribution of pranopfen might be affected by probenecid. However, probenecid has only a slight effect on the tissue distribution of pranopfen (Table 3). It has been reported that the apparent K<sub>i</sub> value for inhibition of *p*-aminohippic acid and ochratoxin A uptake by probenecid is 35 ± 7.9 µM and 30.5 ± 7.9 µM in rabbit renal proximal tubules, respectively.<sup>22</sup> Furthermore, the K<sub>i</sub> value of probenecid for human organic transporter was 44–766 µM using mouse proximal tubule cell stably expressing human organic anion transporter 2 (hOAT2) and hOAT4.<sup>18</sup> The plasma concentration of probenecid was 10–20 µg/ml (35–70 µM, in Fig. 1). The free plasma concentration of probenecid was estimated to be 5.3–10.5 µM based on an 85% binding to rabbit plasma protein.<sup>23</sup> Therefore, it appears that the effect of probenecid on the tissue transport of pranopfen via an active transporter is negligible due to the low plasma concentration of probenecid.

#### Inhibition of Pranopfen Glucuronide Formation by Probenecid

Most NSAIDs, including 2-aryl propionic acids, are eliminated primarily by conjugation with glucuronic acid, with varying degrees of phase 1 metabolism. Furthermore, a major route of elimination for probenecid is also conjugation with glucuronic acid,<sup>24</sup> which may competitively decrease pranopfen glucuronide formation. The effect of probenecid on the glucuronidation of pranopfen was estimated in kidney microsomes. Although pranopfen glucuronide is unstable at pH 7.4 due to an acyl migration on

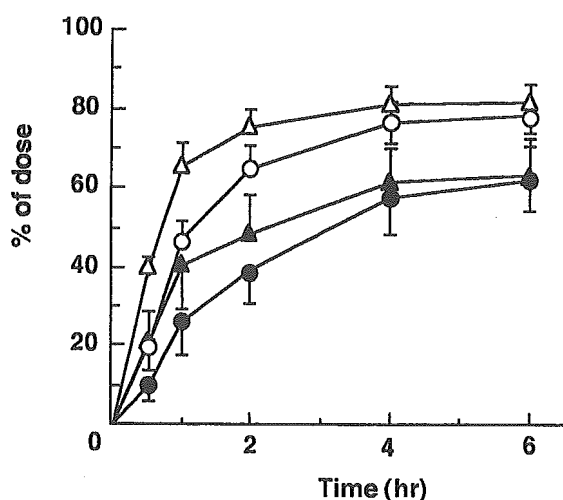


**Fig. 3.** Effect of probenecid on the cumulative urinary extraction of S(+) and (-)-(R)-pranopfen after an i.v. bolus injection of racemic pranopfen in rabbits. Values represent the mean ± SD (n = 3). (+)-(S)-pranopfen: ○, without probenecid; ●, with probenecid. (-)-(R)-pranopfen: △, without probenecid; ▲, with probenecid. Dose: 5 mg/kg of pranopfen and 100 mg/kg of probenecid.

**TABLE 2. Effect of probenecid on the protein binding of pranopfen in rabbit plasma**

| Concentration of probenecid (µg/ml) | Binding %         |                   | S/R ratio |
|-------------------------------------|-------------------|-------------------|-----------|
|                                     | (-)-(R)-pranopfen | (+)-(S)-pranopfen |           |
| 0                                   | 97.2              | 98.5              | 1.02      |
| 100                                 | 97.7              | 98.5              | 1.01      |
| 200                                 | 95.9              | 97.5              | 1.02      |
| 300                                 | 96.2              | 97.6              | 1.02      |

TABLE 3. Effect of probenecid on tissue distribution of (+)-(S)- and (-)-(R)-pranoprofen at 45 min after intravenous bolus injection of 5 mg/kg racemic pranoprofen

| Tissue | Relative tissue level |                     |      |                     |                     |      |
|--------|-----------------------|---------------------|------|---------------------|---------------------|------|
|        | Without probenecid    |                     |      | With probenecid     |                     |      |
|        | (+)-(S)-pranoprofen   | (-)-(R)-pranoprofen | S/R  | (+)-(S)-pranoprofen | (-)-(R)-pranoprofen | S/R  |
| Liver  | 0.14 ± 0.01           | 0.17 ± 0.01         | 0.82 | 0.12 ± 0.03         | 0.16 ± 0.04         | 0.75 |
| Kidney | 1.98 ± 0.17           | 6.20 ± 0.60         | 0.32 | 1.71 ± 0.27         | 5.82 ± 1.03         | 0.29 |
| Heart  | 0.29 ± 0.01           | 0.30 ± 0.03         | 0.97 | 0.17 ± 0.04         | 0.19 ± 0.08         | 0.89 |
| Spleen | 0.25 ± 0.01           | 0.33 ± 0.02         | 0.84 | 0.21 ± 0.04         | 0.26 ± 0.03         | 0.81 |
| Lung   | 0.26 ± 0.01           | 0.31 ± 0.03         | 0.84 | 0.34 ± 0.10         | 0.42 ± 0.87         | 0.81 |
| Muscle | 0.074 ± 0.004         | 0.119 ± 0.0009      | 0.59 | 0.049 ± 0.021       | 0.074 ± 0.017       | 0.66 |

glucuronic acid and hydrolysis, the glucuronidation activity was estimated at pH 7.4 in order to compare glucuronide formation of pranoprofen in the presence and absence of probenecid. The glucuronidation activity of pranoprofen decreased with increasing concentration of probenecid, as shown in Figure 4. However, probenecid inhibited glucuronidation of the (-)-(R)- and (+)-(S)-forms to the same extent. When probenecid is present in the kidney at the same concentration as pranoprofen (1 mM), probenecid inhibits about 20% of the activity of conjugation of both pranoprofen enantiomers with glucuronic acid. The  $K_i$  value was roughly calculated, assuming that probenecid competitively inhibits the formation of the pranoprofen conjugate. The  $K_i$  value of probenecid was 460 and 320  $\mu$ M for (-)-(R)- and (+)-(S)-pranoprofen, respectively. Probenecid has been shown to inhibit acetaminophen glucuronidation both competitively ( $K_i = 460 \mu$ M)<sup>25</sup> and uncompetitively ( $K_i = 600 \mu$ M)<sup>12</sup> in rat liver microsomes. The results of the present study indicate a similar  $K_i$  value. Probenecid levels were maintained at around 20  $\mu$ g/ml (70  $\mu$ M) when pranoprofen was administered 90 min after the oral administration of probenecid. The free tissue concentration of probenecid is calculated to be 10.5  $\mu$ M, taking into account an 85% binding to rabbit plasma protein.<sup>23</sup> Therefore, it is likely that probenecid does not inhibit the glucuronidation

of pranoprofen due to the low free tissue concentration of probenecid. However, both pranoprofen and probenecid may accumulate in certain renal tissues through active transport, and then interact with each other during glucuronide formation, although the average renal concentration is not high (Table 2). When probenecid is coadministered, the glucuronidation of pranoprofen might be inhibited. Zomepirac, an NSAID, is also metabolized to the glucuronide and excreted into the urine. Smith et al.<sup>5</sup> reported that probenecid inhibits clearance for the conjugation of zomepirac with glucuronic acid by 71% and the urinary excretion clearance of zomepirac glucuronide by 72%. The renal excretion of pranoprofen glucuronides might also be inhibited by probenecid. Furthermore, the glucuronide might be hydrolyzed to the parent pranoprofen, resulting in an increased plasma concentration.

It has been reported that the elimination of ketoprofen and benoxaprofen is enantioselectively affected by probenecid in a dose-dependent manner.<sup>14</sup> This enantioselective inhibition by probenecid has been explained based on an enhanced unidirectional chiral inversion due to the reduced elimination clearance. However, the disposition of pranoprofen, which did not show unidirectional chiral inversion, was nonenantioselectively affected by probenecid. A lack of unidirectional chiral inversion of pranoprofen and its rapid elimination may minimize the effect of probenecid. Furthermore, the low plasma and tissue concentration of probenecid due to the low dose used might induce only a small effect on pranoprofen disposition.

In conclusion, the observed interaction between pranoprofen and probenecid led to a significant decrease in pranoprofen clearance based on its glucuronidation in the kidney and subsequent excretion of the glucuronide in urine and enantioselective effects were negligible.

#### LITERATURE CITED

1. Brown GR. Cephalosporin-probenecid drug interactions. *Clin Pharmacokinet* 1993;24:289-300.
2. Gimeno MJ, Martinez M, Granero L, Torres-Molina F, Peris JE. Influence of probenecid on the renal excretion mechanisms of cefadroxil. *Drug Metab Dispos* 1996;24:270-272.
3. Resetar A, Minick D, Spector T. Glucuronidation of 3'-azido-3'-deoxythymidine catalyzed by human liver UDP-glucuronosyltransferase. Significance of nucleoside hydrophobicity and inhibition by xenobiotics. *Biochem Pharmacol* 1991;42:559-568.
4. Guarino AM, Conway WD, Fales HM. Mass spectral identification of probenecid metabolites in rat bile. *Eur J Pharmacol* 1969;8:244-252.

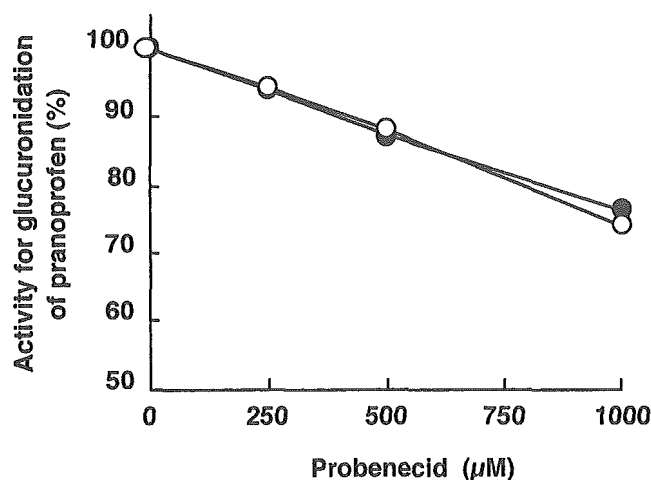


Fig. 4. Effect of probenecid on the activity of pranoprofen glucuronidation  $\bullet$ , (+)-(S)-pranoprofen;  $\circ$ , (-)-(R)-pranoprofen. Pranoprofen was reacted at 1 mM.

5. Smith PC, Langendijk PN, Bosso JA, Benet LZ. Effect of probenecid on the formation and elimination of acyl glucuronides: studies with zomepirac. *Clin Pharmacol Ther* 1985;38:121-127.
6. Spahn H, Spahn I, Benet LZ. Probenecid-induced changes in the clearance of carprofen enantiomers: a preliminary study. *Clin Pharmacol Ther* 1989;45:500-505.
7. Upton RA, Williams RL, Buskin JN, Jones RM. Effects of probenecid on ketoprofen kinetics. *Clin Pharmacol Ther* 1982;31:705-712.
8. Hedaya MA, Elmquist WF, Sawchuk RJ. Probenecid inhibits the metabolic and renal clearances of zidovudine (AZT) in human volunteers. *Pharm Res* 1990;7:411-417.
9. de Miranda P, Good SS, Yarchoan R, Thomas RV, Blum MR, Myers CE, Broder S. Alteration of zidovudine pharmacokinetics by probenecid in patients with AIDS or AIDS-related complex. *Clin Pharmacol Ther* 1989;46:494-500.
10. Kornhauser DM, Petty BG, Hendrix CW, Woods AS, Nerhood LJ, Bartlett JG, Lietman PS. Probenecid and zidovudine metabolism. *Lancet* 1989;2:473-475.
11. Abernethy DR, Greenblatt DJ, Ameer B, Shader RI. Probenecid impairment of acetaminophen and lorazepam clearance: direct inhibition of ether glucuronide formation. *J Pharmacol Exp Ther* 1985;234:345-349.
12. Kamali F. The effect of probenecid on paracetamol metabolism and pharmacokinetics. *Eur J Clin Pharmacol* 1993;45:551-553.
13. Nomura T, Imai T, Otagiri M. Stereoselective disposition of pranoprofen, a nonsteroidal antiinflammatory drug, in rabbits. *Biol Pharm Bull* 1993;16:298-303.
14. Palylyk EL, Jamali F. Ketoprofen-probenecid interaction in the rat: a probenecid concentration-dependent stereoselective process. *J Pharm Sci* 1993;82:296-300.
15. Spahn H, Iwakawa S, Bevet LZ, Lin ET. Influence of probenecid on the urinary excretion rates of the diastereomeric benoxaprofen glucuronides. *Eur J Drug Metab Pharmacokin* 1987;12:233-237.
16. Foster RT, Jamali F, Russell AS. Pharmacokinetics of ketoprofen enantiomers in cholecystectomy patients: influence of probenecid. *Eur J Clin Pharmacol* 1989;37:589-594.
17. Bischer A, Iwaki M, Zia-Amirhosseini P, Benet LZ. Stereoselective reversible binding properties of the glucuronide conjugates of fenoprofen enantiomers to human serum albumin. *Drug Metab Dispos* 1995;23:900-903.
18. Enomoto A, Takeda M, Shimoda M, Narikawa S, Kobayashi Y, Kobayashi Y, Yamamoto T, Sekine T, Cha SH, Niwa T, Endou H. Interaction of human organic anion transporters 2 and 4 with organic anion transport inhibitors. *J Pharmacol Exp Ther* 2002;301:797-802.
19. Sweet DH, Miller DS, Pritchard JB, Fujiwara Y, Beier DR, Nigam SK. Impaired organic anion transport in kidney and choroid plexus of organic anion transporter 3 (Oat3 (Slc22a8)) knockout mice. *J Biol Chem* 2002;277:26934-26943.
20. Masuda S, Saito H, Inui KI. Interactions of nonsteroidal anti-inflammatory drugs with rat renal organic anion transporter, OAT-K1. *J Pharmacol Exp Ther* 1997;283:1039-1042.
21. Cox PG, van Os CH, Russel FG. Accumulation of salicylic acid and indomethacin in isolated proximal tubular cells of the rat kidney. *Pharmacol Res* 1993;27:241-252.
22. Groves CE, Morales M, Wright SH. Peritubular transport of ochratoxin A in rabbit renal proximal tubules. *J Pharmacol Exp Ther* 1998;284:943-948.
23. Watari N, Aizawa K, Kaneniwa N. Dose- and time-dependent kinetics of the renal excretion of nitrofurantoin in the rabbit. *J Pharm Sci* 1985;74:165-170.
24. Cunningham RF, Israili ZH, Dayton PG. Clinical pharmacokinetics of probenecid. *Clin Pharmacokin* 1981;6:135-151.
25. von Moltke LL, Manis M, Harmatz JS, Poorman R, Greenblatt DJ. Inhibition of acetaminophen and lorazepam glucuronidation in vitro by probenecid. *Biopharm Drug Dispos* 1993;14:6119-6130.



## Enantiospecific Disposition of Pranoprofen in Beagle Dogs and Rats

TERUKO IMAI,\* TADAYUKI NOMURA, MAYUMI ASO, AND MASAKI OTAGIRI  
*Faculty of Pharmaceutical Sciences, Kumamoto University, Kumamoto, Japan*

**ABSTRACT** The pharmacokinetic characteristics of pranoprofen enantiomer were examined and compared with the disposition of the corresponding isomer after the administration of racemic pranoprofen to beagle dogs and rats. The plasma levels of (+)-(S)-isomer were significantly higher than those of (–)-(R)-isomer in dogs and rats by either intravenous or oral administration. Although the oral bioavailability and absorption rate constant between the (–)-(R)- and (+)-(S)-form was the same, the elimination rate constant of the (+)-(S)-form was significantly lower than that of the (–)-(R)-form in both dogs and rats. This discrepancy can be explained on the basis of differences in protein binding and the metabolism of the two enantiomers. The (–)-(R)-isomer was predominantly conjugated depending on its higher free plasma level and its faster metabolic rate than the (+)-(S)-form, and thus was excreted more rapidly in the urine and bile in the form of pranoprofen glucuronide. Furthermore, a (–)-(R)- to (+)-(S)-inversion occurred to the extent of 14% in beagle dogs, but not in rats. This chiral inversion might be an important factor in the slow elimination of the (+)-(S)-form in dogs. The most efficient organ for chiral inversion was the liver, followed by kidney and intestine. *Chirality* 15:312–317, 2003. © 2003 Wiley-Liss, Inc.

**KEY WORDS:** 2-arylpropionic acid; plasma concentration; chiral inversion; acyl glucuronidation; protein binding

The 2-arylpropionic acids (2-APA) or “profens” are an important group of nonsteroidal antiinflammatory drugs, and are both widely prescribed and generally perceived to be of considerable benefit in diseases such as arthritis and rheumatism. Although profens contain a chiral center and exhibit optical activity, 2-APA, with the exception of naproxen, is administered clinically in the racemic form. In general, enantiomers have very similar physicochemical properties, but they frequently show quite different pharmacological and pharmaceutical properties. It is well known that stereoisomers may differ in terms of their absorption, distribution, metabolism, and excretion,<sup>1</sup> particularly when these processes involve the interaction of the drug with chiral macromolecules such as transporters and enzymes. Furthermore, some 2-APA, e.g., ibuprofen and fenoprofen, but not all members of this class, undergo a substantial *in vivo* unidirectional bioinversion whereby the inactive (–)-(R)-isomer is converted into its active antipode.<sup>2</sup> The extent to which this inversion occurs differs, depending on the individual drug and the species studied.<sup>2,3</sup>

Pranoprofen (2-5H-[1]benzopyrano[2,3-b]pyridine-7-yl)propionic acid (Fig. 1) is a 2-APA derivative used as a racemic mixture. We previously reported the disposition of pranoprofen enantiomers in rabbits.<sup>4</sup> The rabbit plasma concentration of the (+)-(S)-isomer was higher than the antipode due to its slower rate of elimination. The (–)-(R)-isomer was predominantly conjugated to acyl glucuronide depending on its higher free plasma level and its faster

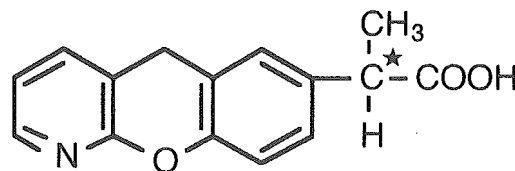


Fig. 1. Chemical structure of pranoprofen.

metabolic rate than the (+)-(S)-form, and thus was rapidly excreted from the kidney as the acyl glucuronide. Furthermore, the (–)-(R)- and (+)-(S)-isoforms interacted with each other in the elimination process through the metabolic pathway to their acyl glucuronide, resulting in different plasma concentration profiles for the administration of the racemate vis-à-vis the individual enantiomers.

The present work was undertaken to study species differences in the stereoselective disposition of pranoprofen. The pharmacokinetic characteristics after the administration of each enantiomer were examined and compared with the disposition of the corresponding isomer after administration of racemic pranoprofen.

This paper was presented at the Symposium on Molecular Chirality 2003 in Kumamoto, Japan.

\*Correspondence to: Prof. Teruko Imai, Faculty of Pharmaceutical Sciences, Kumamoto University, 5-1 Oe-honmachi, Kumamoto, 862-0973 Japan. E-mail: iteruko@gpo.kumamoto-u.ac.jp

Received for publication 21 August 2002; Accepted 5 November 2002  
 Published online 5 March 2003 in Wiley InterScience  
 (www.interscience.wiley.com). DOI: 10.1002/chir.10207

## EXPERIMENTAL

### Materials

Racemic pranoprofen and its enantiomers were kindly donated by Mitsubishi Welfide Co. (Tokyo, Japan). The optical purity of (+)-(S)- and (-)-(R)-isomers were 98.4 and 97.9%, respectively. Coenzyme A (CoA) and ATP-Na were purchased from Sigma Chemical Co. (St. Louis, MO). All other chemicals and solvents were of an analytical grade.

### Animals

Male Wistar rats (8 weeks, 230–270 g) and beagle dogs (3–5 years, 11–13 kg) were used. Rats were fasted for 12 h and cannulation was then done from the jugular vein into the right atrium using a silicone tube (0.3 mm outside diameter) under ether anesthesia. After 3 days the rats were again fasted for 12 h and pranoprofen (5 mg/kg for the racemate), suspended in 5% gum arabic, was administered into the stomach via a catheter. A phosphate buffer solution of racemic pranoprofen (5 mg/kg) and enantiomers (2.5 mg/kg) was administered i.v. into the catheter. At appropriate intervals blood samples were withdrawn into a heparinized syringe from the silicon cannulation tube. Dogs were used in a crossover manner with intervals of 2 weeks for washout. The dogs were on a liquid diet (Besvion®, Fujisawa Pharm. Co., Osaka, Japan) for 2 days followed by fasting for 12 h with water ad libitum prior to drug administration. A pranoprofen sample (5 mg/kg for the racemate) suspended in 5% gum arabic was administered into the stomach through a rubber tube. In the case of i.v. administration, a solution of pranoprofen in a phosphate buffer was administered into the cephalic vein (5 mg/kg for the racemate, 2.5 mg/kg for the enantiomer). Blood samples were withdrawn into heparinized syringes from the cephalic vein in the other foot. The blood samples were immediately centrifuged at 3,000 rpm to obtain plasma. The plasma was acidified to below pH 3.5 by adding the same volume of 0.1 M citrate buffer (pH 3.0) to prevent hydrolysis of the glucuronide.

### Sample Treatment and Assay

(+)-(S)- and (-)-(R)-pranoprofen in plasma were determined by a previously described HPLC method.<sup>4</sup> One-half ml of 1 M HCl was added to the plasma sample (1 ml) adjusted to below pH 3.5 and the pranoprofen was extracted with 6 ml of ether. The evaporated residue from the ether phase was dissolved in the HPLC mobile phase and injected into the HPLC. Methyl *p*-aminobenzoate was used as an internal standard. The HPLC assay was performed on a Chiralcel OJ column (25 × 2.6 mm i.d., Dical Chemical Industries, Tokyo, Japan) with a mobile phase comprised of *n*-heptan:2-propanol:acetic acid (70:40:1), pumped at a flow rate of 1.0 ml/min using a Hitachi 655A-11 pump equipped with a Hitachi D-2500 chromatointegrator (Tokyo, Japan). The fluorescence of each enantiomer was detected at an excitation wavelength 250 nm and an emission at 330 nm.

### Ultrafiltration of Plasma

The free fraction of pranoprofen in plasma was measured by ultrafiltration using a micropartition system MPS-1

(Amicon Co., Danvers, MA) fitted with a membrane filter with molecular weight cutoff value of 30,000. The plasma sample, containing 10–100 µg/ml of pranoprofen, was applied to the reservoir and centrifuged at 2,000g for 10 min at 37°C. After centrifugation the filtrate was analyzed by HPLC.

### Chiral Inversion in Tissue Slices

Dogs were sacrificed by exsanguination under ether anesthesia and tissues were removed and stored on an ice bath in a beaker containing Krebs-Ringer bicarbonate buffer with 0.2% glucose. Each tissue was sliced with a razor blade to about 1 mm in thickness. The small intestine was removed and the contents were washed with buffer, the tube was then opened and resuspended in Krebs-Ringer bicarbonate buffer, blotted on a filter paper, and sliced.

A tissue slice (100 mg) was added to 5 ml of Krebs-Ringer bicarbonate buffer containing 1 mM of CoA, 5 mM of ATP-Na, and 50 µM of MgSO<sub>4</sub>, then bubbled with an O<sub>2</sub>:CO<sub>2</sub> (95:5) gas mixture for 5 min. Then 100 µM (-)-(R)-pranoprofen was added and incubated at 37°C for 30 min. The concentration of (+)-(S)-pranoprofen produced by inversion of the (-)-(R)-form was assayed by HPLC as described above.

### Pharmacokinetic Analysis Methods

The plasma concentration profile after the oral administration of pranoprofen was analyzed using a two-compartment model. The area under the plasma concentration time curve (AUC) was calculated by the trapezoidal method and the terminal exponential slope, obtained from a linear regression of the log-linear portion. The total clearance was estimated by dose/AUC.

## RESULTS AND DISCUSSION

Figure 2 shows the time-course for the plasma concentration of (+)-(S)- and (-)-(R)-pranoprofen after oral and i.v. administration of a racemic mixture to dogs and rats. The pharmacokinetic parameters are listed in Table 1. For both administration routes, plasma levels of the (+)-(S)-isomer were significantly higher than those of the (-)-(R)-isomer in both dogs and rats. As shown in Table 1, the S/R ratio of AUC after i.v. administration was 1.67 and 3.29 for rats and dogs, respectively. The oral bioavailability of each enantiomer, calculated from the ratio of AUC<sub>po</sub> against AUC<sub>iv</sub> for the (-)-(R)- and (+)-(S)-form remained unchanged (0.71–0.73 for rats, 0.95–0.97 for dogs). Furthermore, the absorption rate constant (*k*<sub>a</sub>) was nearly the same for each isomer. These data suggest that the absorption of pranoprofen through the gastrointestinal tract was nonstereoselective and that no stereoselective presystemic metabolism occurred. It has recently been reported that the intestinal absorption of several compounds is mediated by specific transporters such as peptide transporters and organic anion transporters<sup>5</sup> and also secreted by efflux transporters such as the P-glycoprotein.<sup>6,7</sup> Although these transporters recognize the configuration of a substrate structure,<sup>8,9</sup> the fact that pranoprofen is nonstereoselec-

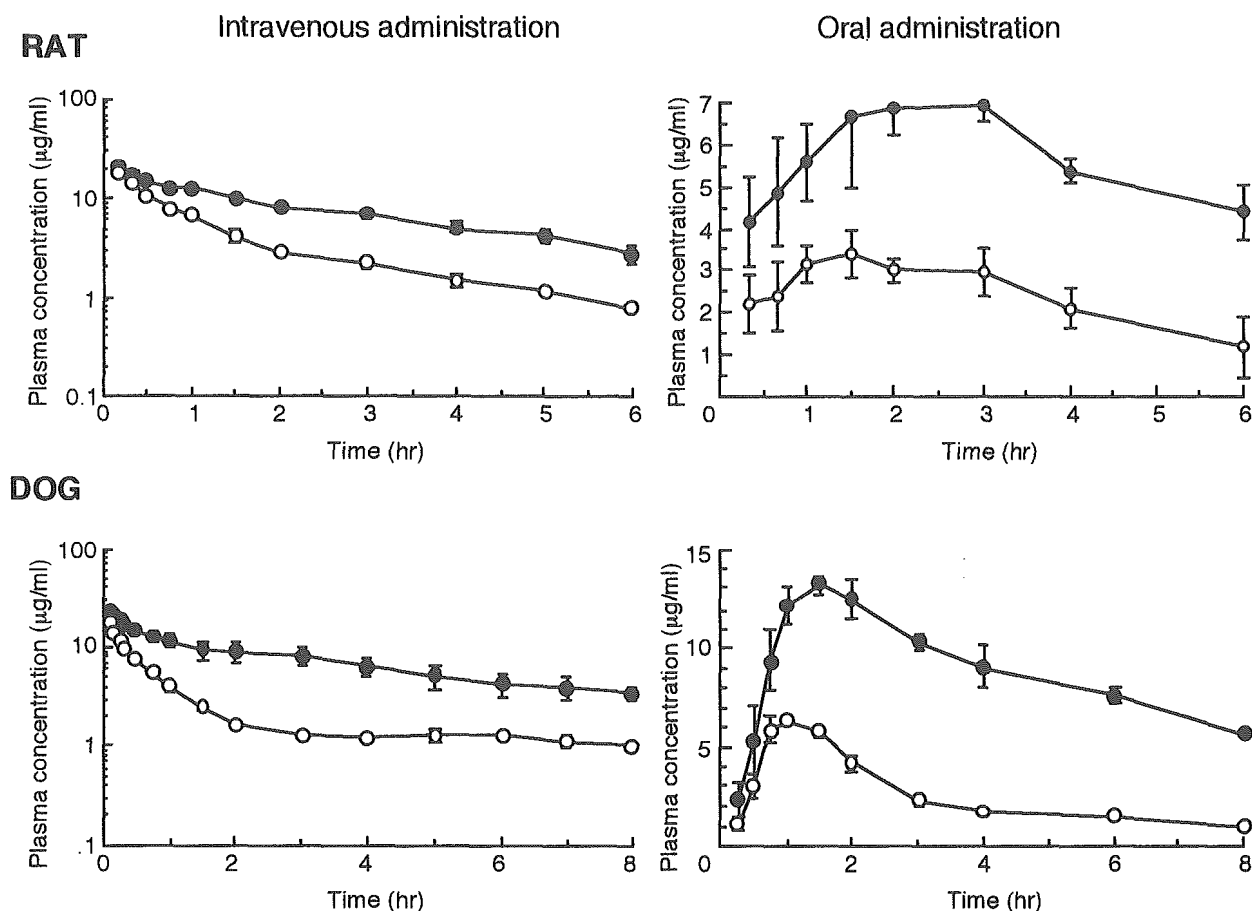


Fig. 2. Plasma concentration of (+)-(S)- and (-)-(R)-pranopfen after oral (right) and i.v. bolus (left) administration of 5 mg/kg of racemic pranopfen to rats (upper) and dogs (lower) ●: (+)-(S)-pranopfen, ○: (-)-(R)-pranopfen. Values represent the mean  $\pm$  SE ( $n = 3-4$ ).

tively absorbed from the gastrointestinal tract indicates that a specific transporter, if present, does not recognize the configuration of pranopfen and/or that pranopfen is mainly absorbed by simple diffusion.

In contrast, the elimination rate constant ( $k_e$ ) for the (+)-(S)-isomer was significantly smaller than that of (-)-(R)-isomer in both dogs and rats. The slow elimination rate of the (+)-(S)-isomer results in high plasma concentrations of the (+)-(S)-isomer. Several possible explanations exist for the rapid elimination of (-)-(R)-pranopfen. First, the me-

tabolism of the (-)-(R)-isomer is faster than the (+)-(S)-isomer. Second, the (+)-(S)-isomer is preferentially provided to the entero-hepatic circulation. Third, the R(-)-isoform is converted to the (+)-(S)-form in the body. It has been reported that pranopfen is detoxified by conversion to the acyl glucuronide and is then excreted into the urine and bile in several species.<sup>10</sup> The total clearance (CL<sub>tot</sub>) for (+)-(S)- and (-)-(R)-pranopfen was determined to be 0.929 and 1.57 for rats, and 0.741 and 2.35 ml/min/kg for dogs, as shown in Table 1. These values are much smaller

TABLE 1. Pharmacokinetic parameters of (+)-(S)- and (-)-(R)-pranopfen after oral and i.v. bolus administration of 5 mg/kg of racemate

|  | Rat              |                    | Dog               |                    |
|--|------------------|--------------------|-------------------|--------------------|
|  | (+)-(S)-isomer   | (-)-(R)-isomer     | (+)-(S)-isomer    | (-)-(R)-isomer     |
| $k_a$ ( $h^{-1}$ )                       | $0.543 \pm 0.08$ | $0.586 \pm 0.05$   | $1.11 \pm 0.17$   | $1.22 \pm 0.26$    |
| $k_e$ ( $h^{-1}$ )                       | $0.503 \pm 0.04$ | $0.916 \pm 0.06^*$ | $0.251 \pm 0.13$  | $0.689 \pm 0.03^*$ |
| V <sub>c</sub> (ml)                      | $21.5 \pm 1.98$  | $23.0 \pm 0.48$    | $1200 \pm 14.7$   | $1450 \pm 99.7$    |
| AUC <sub>iv</sub> ( $\mu g \cdot h/ml$ ) | $44.6 \pm 3.01$  | $26.6 \pm 1.59^*$  | $58.3 \pm 9.6$    | $17.7 \pm 0.89^*$  |
| CL <sub>tot</sub> (ml/min/kg)            | $0.929 \pm 0.05$ | $1.57 \pm 0.10^*$  | $0.741 \pm 0.119$ | $2.35 \pm 0.131^*$ |
| AUC <sub>po</sub> ( $\mu g \cdot h/ml$ ) | $32.5 \pm 1.98$  | $19.9 \pm 1.81^*$  | $55.2 \pm 1.58$   | $17.1 \pm 0.88^*$  |
| AUC <sub>po</sub> /AUC <sub>iv</sub>     | 0.729            | 0.748              | 0.947             | 0.966              |

Values represent the mean  $\pm$  SD ( $n = 3-4$ ).

\* $P < 0.05$  vs. (+)-(S)-form.

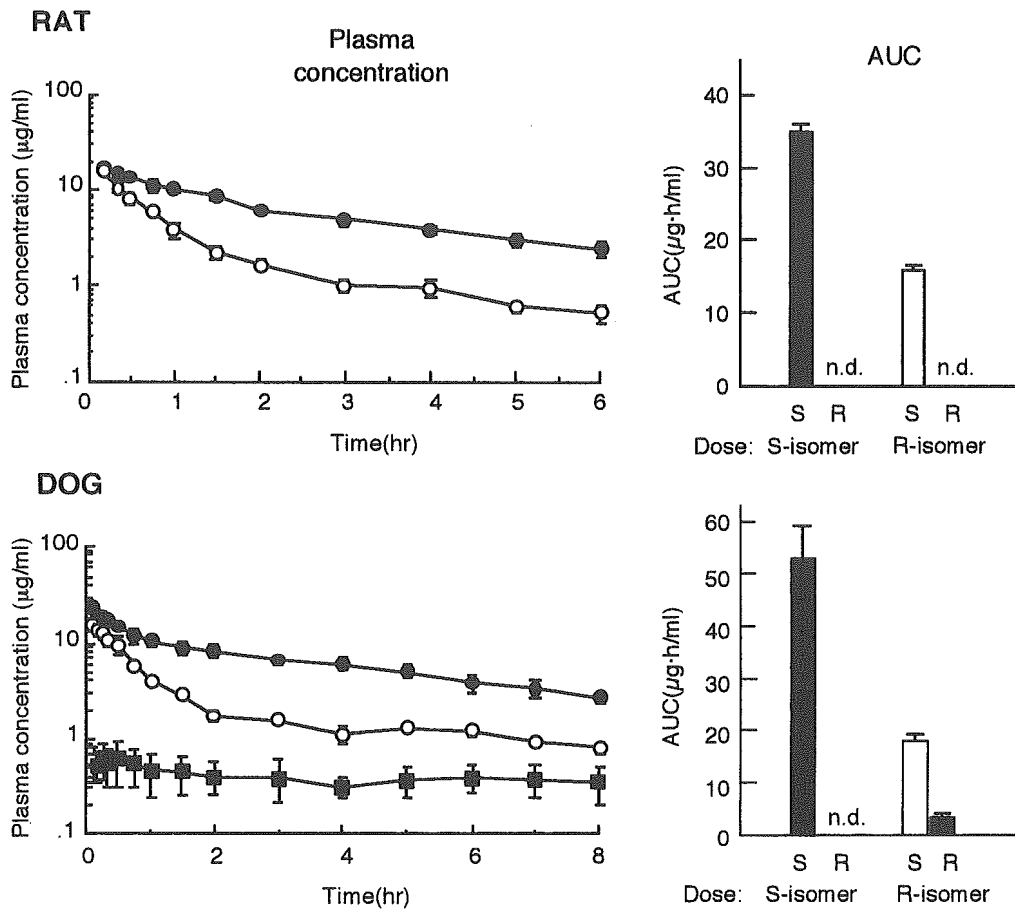


Fig. 3. Plasma concentrations and AUC of (+)-(S)- and (-)-(R)-pranopfen after the administration of an i.v. bolus of 2.5 mg/kg of each enantiomer to rats and dogs. Values represent the mean  $\pm$  SE ( $n = 3-4$ ). For plasma concentration  $\bullet$ : (+)-(S)-pranopfen,  $\circ$ : (-)-(R)-pranopfen,  $\blacksquare$ : (+)-(S)-pranopfen inverted from (-)-(R)-pranopfen. For AUC  $\blacksquare$ : (+)-(S)-pranopfen,  $\square$ : (-)-(R)-pranopfen.

than the hepatic blood flow, indicating that pranopfen is metabolized to its glucuronide at a rate limited by the enzyme activity. In general, since a  $CL_{tot}$  of a low clearance drug can be briefly represented as  $f \cdot CL_{int}$ , the free fraction of pranopfen in plasma ( $f$ ) is an important factor in determining  $CL_{tot}$ . Therefore, the free fraction of pranopfen in plasma was measured by ultrafiltration. The free fraction of (+)-(S)-pranopfen in rat plasma was 0.4–0.7%, whereas that of (-)-(R)-isomer was 0.8–1.0% in the presence of 10–100  $\mu\text{g/ml}$  of racemic pranopfen. In addition, the free fraction of (+)-(S)- and (-)-(R)-pranopfen in dog

plasma was in the range of 0.5–0.9% and 1.0–1.6%, respectively. Previously, the (+)-(S)-preferential binding of pranopfen to human plasma was explained by stereoselective binding to human serum albumin through the interaction of the carboxylic acid group to the Site II binding site.<sup>11</sup> The stereoselective binding to plasma proteins of dogs and rats might depend on the binding affinity of each isomer to albumin. These data suggest that the higher free fraction of (-)-(R)-isomer in rat and dog plasma might induce the faster metabolism of the (-)-(R)-isomer than the (+)-(S)-isomer.

TABLE 2. Pharmacokinetic parameters of (+)-(S)- and (-)-(R)-pranopfen after oral and i.v. bolus administration of 2.5 mg/kg of each enantiomer

|   | Rat             |                   | Dog              |                   |  |
|---|-----------------|-------------------|------------------|-------------------|--|
|   | (+)-(S)-form    | (-)-(R)-form      | (+)-(S)-form     | (-)-(R)-form      | (-)-(R) $\rightarrow$ (+)-(S) <sup>a</sup> |
| $k_e$ ( $\text{h}^{-1}$ )               | $0.47 \pm 0.01$ | $0.95 \pm 0.05^b$ | $0.31 \pm 0.02$  | $0.70 \pm 0.04^b$ |  |
| $V_c$ (ml)                              | $27.1 \pm 1.09$ | $25.2 \pm 3.41$   | $1230 \pm 62.6$  | $1400 \pm 72.0$   |  |
| AUC ( $\mu\text{g} \cdot \text{h/ml}$ ) | $34.4 \pm 1.72$ | $16.8 \pm 1.21^b$ | $53.2 \pm 6.31$  | $18.4 \pm 1.72^b$ | $3.21 \pm 1.20$                            |
| $CL_{tot}$ (ml/min/kg)                  | $1.21 \pm 0.06$ | $2.48 \pm 0.17^b$ | $0.780 \pm 0.08$ | $1.93 \pm 0.23^b$ |  |

Values represent the mean  $\pm$  SD ( $n = 3-4$ ).

<sup>a</sup>Chiral inversion from (-)-(R)-pranopfen.

<sup>b</sup> $P < 0.05$  vs. (+)-(S)-form.

Percent of inversion =  $\text{AUC}(\text{R} \rightarrow \text{S}) / (\text{AUC}(\text{R}) + \text{AUC}(\text{R} \rightarrow \text{S})) \times 100 = 14\%$ .

Furthermore, we previously reported that pranoprofen is (-)-(R)-preferentially metabolized to the acyl glucuronide in the rabbit liver and kidney.<sup>4</sup> However, very slow glucuronidation was observed in rabbit liver due to the rapid hydrolysis of pranoprofen glucuronide for both enantiomers ( $t_{1/2} = 25$  min for (+)-(S)-isomer,  $t_{1/2} = 15$  min for (-)-(R)-isomer).<sup>4</sup> On the other hand, pranoprofen was (-)-(R)-preferentially metabolized to the acyl glucuronide in rabbit kidney microsomes, where pranoprofen glucuronide was stable ( $t_{1/2} \approx 2.5$  h for both (-)-(R)- and (+)-(S)-isomers).<sup>4</sup> The  $V_{max}$  value of (-)-(R)-pranoprofen glucuronidation was 5.7-fold greater than that of (+)-(S)-enantiomer in rabbit kidney microsomes, in spite of nearly the same  $K_m$  value for each enantiomer.<sup>4</sup> Unfortunately, further metabolic experiments have not been performed using tissue microsomes in rats and dogs. However, (-)-(R)-pranoprofen may be rapidly metabolized in rats and dogs, although the substrate specificity for UDP-glucuronosyl transferase isozyme in different species is unclear. In addition to the glucuronidation activity toward (-)-(R)-pranoprofen, its higher free fraction in plasma might enhance the (-)-(R)-selective elimination in dogs and rats.

It has been reported that the long half-life of pranoprofen in rats is attributable to the entero-hepatic circulation by extensive biliary excretion.<sup>12</sup> The enhanced biliary excretion of the (+)-(S)-enantiomer may contribute to the longer terminal half-life due to reabsorption from intestine. Menzel et al.<sup>13</sup> reported that (+)-(S)-ketoprofen and (+)-(S)-ibuprofen were more extensively excreted in the bile than the (-)-(R)-enantiomer and that nearly the entire amount of (+)-(S)-enantiomer excreted in the bile was reabsorbed, compared to a low amount for the (-)-(R)-enantiomer. The reasons for the substance-dependent stereoselective reabsorption may be the stereoselective hydrolysis of the acyl glucuronide in the intestine and/or a chiral inversion in the intestine. Since entero-hepatic circulation is important for the stereoselective pharmacokinetics of 2-APA, further experiments will be needed.

The chiral inversion of pranoprofen was studied. Figure 3 shows the plasma concentration profile of pranoprofen after i.v. administration of each enantiomer in rats and dogs; the pharmacokinetic parameters are listed in Table 2. Interestingly, the (+)-(S)-isomer was detected after administration of the (-)-(R)-enantiomer in dogs. However, a chiral inversion from the (+)-(S)- to (-)-(R)-form was not observed. The percentage of chiral inversion from (-)-(R)- to (+)-(S)-isomer in dogs was found to be 14%. The (-)-(R)- to (+)-(S)-inversion might be attributed to the high plasma concentration of the (+)-(S)-isomer in dogs. In contrast, a chiral inversion was not observed in rats. We previously found an absence of any chiral inversion in rabbits.<sup>4</sup> The (-)-(R)- to (+)-(S)-enantiomer inversion of pranoprofen is specific to beagle dogs. Some members of the 2-APA family, such as ibuprofen and fenoprofen, undergo substantial unidirectional inversion of configuration about the chiral center.<sup>2,3</sup> The proposed mechanism of the R- to S-enantiomer inversion of 2-APA involves the stereoselective formation of a thioester with CoA and subsequent racemization (or inversion) and hydrolysis to generate the free acid.<sup>14,15</sup> Knadler and Hall<sup>16</sup> reported that the formation of

**TABLE 3. Chiral inversion from (-)-(R)-pranoprofen (100  $\mu$ M) to (+)-(S)-form in various tissue slices of dog**

| Tissues         | (+)-(S)-pranoprofen inverted from (-)-(R)-enantiomer ( $\mu$ M) |
|-----------------|---|
| Liver           | 4.04  |
| Kidney          | 0.98  |
| Small intestine | 0.50  |

CoA thioesters can account for the stereoselectivity and substrate specificity of inversion. The species difference for the chiral inversion of pranoprofen can be attributed, in part, to a discrepancy in the fatty acyl CoA synthetase isozyme.

Table 3 shows the percentage of (-)-(R)- to (+)-(S)-pranoprofen inversion in several tissues of beagle dogs. The most efficient site for chiral inversion was the liver, followed by the kidney and intestine, analogous to the distribution of fatty acyl-CoA synthetase.<sup>17</sup> These observations suggest that thioester formation with CoA might account for the (-)-(R)- to (+)-(S)-inversion of pranoprofen. The intestine is an important organ for the presystemic inversion of a 2-APA derivatives, such as fenoprofen.<sup>18</sup> However, the fact that the absorption of pranoprofen was not stereoselective after oral administration of the racemate in dogs indicated that such low activity for chiral inversion in the intestine was not important in the absorption of pranoprofen.

Moreover, the pharmacokinetic parameters after administration of each enantiomer were similar to those of racemate dosing in rats and dogs, except the  $CL_{tot}$  value for the (-)-(R)-isomer in rats. Our previous data have demonstrated that an interaction of (-)-(R)- and (+)-(S)-pranoprofen in acyl glucuronidation in rabbit kidney results in the slower elimination of each isomer after the administration of racemate, compared to enantiomer.<sup>4</sup> The present data show that an interaction of each enantiomer in an elimination process was not found in dogs and rats, possibly due to the low enzymatic activity of acyl glucuronidation.

In conclusion, the disposition of pranoprofen enantiomers in rats and beagle dogs was found to be different, especially with respect to the elimination process. This can be explained on the basis of differences in protein binding and the metabolic activity of these two enantiomers. The (-)-(R)-isomer was predominantly conjugated depending on its higher free plasma level and its faster metabolic rate than the (+)-(S)-form, and thus was rapidly excreted in the urine and bile in the form of pranoprofen glucuronide. Furthermore, the (-)-(R)- to (+)-(S)-inversion that occurs in beagle dogs might be an important factor in the slow elimination of the (+)-(S)-form in dogs.

#### LITERATURE CITED

- Jamali F, Mehvar R, Pasutto M. Enantioselective aspects of drug action and disposition: therapeutic pitfalls. *J Pharm Sci* 1989;78:695-715.
- Caldwell J, Hutt AJ, Fournel-Gigleux S. The metabolic chiral inversion and dispositional enantioselectivity of the 2-arylpropionic acids and their biological consequences. *Biochem Pharmacol* 1988;37:105-114.

3. Jamali F. Pharmacokinetics of enantiomers of chiral non-steroidal anti-inflammatory drugs. *Eur J Drug Metab Pharmacokinet* 1988;13:1-9.
4. Nomura T, Imai T, Otagiri M. Stereoselective disposition of pranoprofen, a nonsteroidal antiinflammatory drug, in rabbits. *Biol Pharm Bull* 1993;16:298-303.
5. Tsuji A, Tamai I. Carrier-mediated intestinal transport of drugs. *Pharm Res* 1996;13:963-977.
6. Stephens RH, O'Neill CA, Warhurst A, Carlson GL, Rowland M, Warhurst G. Kinetic profiling of P-glycoprotein-mediated drug efflux in rat and human intestinal epithelia. *J Pharmacol Exp Ther* 2001;296:584-591.
7. Suzuki H, Sugiyama Y. Role of metabolic enzymes and efflux transporters in the absorption of drugs from the small intestine. *Eur J Pharm Sci* 2000;12:3-12.
8. Daniel H, Morse EL, Adibi SA. Determinants of substrate affinity for the oligopeptide/H<sup>+</sup> symporter in the renal brush border membrane. *J Biol Chem* 1992;267:9565-9573.
9. Ogihara T, Tamai I, Takanaga H, Sai Y, Tsuji A. Stereoselective and carrier-mediated transport of monocarboxylic acids across Caco-2 cells. *Pharm Res* 1996;13:1828-1832.
10. Arima N, Kato Y. Species differences in absorption, metabolism and excretion of pranoprofen, a 2-arylpropionic acid derivative, in experimental animals. *J Pharmacobiodyn* 1990;13:739-744.
11. Nomura T, Sakamoto K, Imai T, Otagiri M. Study of interaction of pranoprofen with human serum albumin: binding properties of enantiomers and metabolite. *J Pharmacobiodyn* 1992;15:589-596.
12. Kato Y, Arima N, Nishimine H. Studies on anti-inflammatory agents. XXXIII. Isolation and identification of the urinary metabolites of 2-(5H-[1]benzopyrano[2,3-b]-pyridin-7-yl)propionic acid (Y-8004) in mice (author's transl.). *Yakugaku Zasshi* 1976;96:941-944.
13. Menzel S, Beck WS, Brune K, Geisslinger G. Stereoselectivity of biliary excretion of 2-arylpropionates in rats. *Chirality* 1993;5:422-427.
14. Hutt AJ, Caldwell J. The metabolic chiral inversion of 2-arylpropionic acids—a novel route with pharmacological consequences. *J Pharm Pharmacol* 1983;35:693-704.
15. Nakamura Y, Yamaguchi T, Takahashi S, Hashimoto S, Iwatani K, Nakagawa Y. Optical isomerization mechanism of R(-)-hydrotropic acid derivatives. *J Pharmacobiodyn* 1981;4:S-1.
16. Knadler MP, Hall SD. Stereoselective arylpropionyl-CoA thioester formation in vitro. *Chirality* 1990;2:67-73.
17. Aas M. Organ and subcellular distribution of fatty acid activating enzymes in the rat. *Biochim Biophys Acta* 1971;231:32-47.
18. Berry BW, Jamali F. Presystemic and systemic chiral inversion of (-)-(R)-fenoprofen in the rat. *J Pharmacol Exp Ther* 1991;258:695-701.



## Cloning, expression and tissue distribution of a tetrameric form of pig carbonyl reductase

Noriyuki Usami<sup>a</sup>, Shuhei Ishikura<sup>a</sup>, Hiroko Abe<sup>a</sup>, Makoto Nagano<sup>a</sup>,  
Miki Uebuchi<sup>b</sup>, Akihiko Kuniyasu<sup>b</sup>, Masaki Otagiri<sup>b</sup>, Hitoshi Nakayama<sup>b</sup>,  
Yorishige Imamura<sup>b</sup>, Akira Hara<sup>a,\*</sup>

<sup>a</sup> Biochemistry Laboratory, Gifu Pharmaceutical University, Mitahora-higashi, Gifu 502-8585, Japan

<sup>b</sup> Faculty of Pharmaceutical Sciences, Kumamoto University, Oe-honmachi, Kumamoto 862-0973, Japan

### Abstract

In this study, we isolated a cDNA for tetrameric carbonyl reductase (CR) from pig heart. The pig CR showed high amino acid sequence identity (81%) with rabbit NADP<sup>+</sup>-dependent retinol dehydrogenase (NDRD). The purified recombinant pig CR and NDRD were about 100-kDa homotetramers and exhibited high reductase activity towards alkyl phenyl ketones,  $\alpha$ -dicarbonyl compounds and all-*trans*-retinal. The identity of NDRD with the tetrameric CR was verified by protein sequencing of CR purified from rabbit heart. Both tetrameric CR and its mRNA were ubiquitously expressed in pig and rabbit tissues. The pig and rabbit enzymes belonged to the short-chain dehydrogenase/reductase family, and their sequences comprise a C-terminal SRL tripeptide, which is a variant of the type 1 peroxisomal targeting signal, SKL. Transfection of HeLa cells with vectors expressing pig CR demonstrated that the enzyme is localized in the peroxisomes. Thus, the tetrameric form of CR represents the first mammalian peroxisomal enzyme that reduces all-*trans*-retinal as the endogenous substrate.

© 2002 Elsevier Science Ireland Ltd. All rights reserved.

**Keywords:** Carbonyl reductase; Short-chain dehydrogenase/reductase family; Retinal reductase; Peroxisomal-targeting signal

### 1. Introduction

Carbonyl reductase (CR, EC 1.1.1.184) catalyzes the NAD(P)H-linked reduction of a variety of carbonyl compounds to their corresponding secondary alcohols [1]. In mammalian tissues the enzyme exists in multiple forms, which are distributed in the mitochondria, microsomes and/or

cytosol of cells. Many mammalian CRs are cytosolic, monomeric reductases with molecular weights of around 34 kDa. The monomeric CRs of humans [2], pig [3] and rabbit [4] belong to the short-chain dehydrogenase/reductase (SDR) family [5], and isatin and 20-ketosteroids have been suggested to be the endogenous substrates of the enzymes of humans [6] and pig [3], respectively. The mitochondrial CRs have been isolated from mouse, guinea pig and pig lungs [7–9] and hamster testis and epididymis [10]. The enzymes also belong to the SDR family [10–12], but are tetra-

\* Corresponding author. Fax: +81-58-237-8586

E-mail address: [hara@gifu-pu.ac.jp](mailto:hara@gifu-pu.ac.jp) (A. Hara).

meric and efficiently reduce endogenous 3-ketosteroids and carbonyl compounds derived from lipid peroxidation. At least two types of CR have been detected in the microsomes of mammalian tissues. One type is identified as 11 $\beta$ -hydroxysteroid dehydrogenase type 1 [13], which is a member of the SDR family. Another type is a male-specific microsomal enzyme in rat liver and kidney [14], and has been thought to be 20 $\beta$ -hydroxysteroid dehydrogenase [15]. In addition to the multiple forms of CR, oligomeric and soluble forms of CR have been isolated from heart [16] and liver [17] of rabbit and dog liver [18]. While the properties of the oligomeric enzymes differ from those of the monomeric and mitochondrial tetrameric CRs, their amino acid sequences, endogenous substrates, tissue distribution and subcellular localization remain unclear.

In the course of searching the tetrameric CR similar to rabbit heart CR (RaCR) [16] in hearts of animals other than rabbits, we found that pig heart contained such an enzyme. In this study, we have purified the pig heart CR (PHCR) as well as RaCR, and determined sequences of peptides derived from the two enzymes. The peptide sequences of RaCR completely matched the regions of the amino acid sequence deduced from a cDNA for rabbit NADP<sup>+</sup>-dependent retinol dehydrogenase (NDRD), which has recently been deposited in the GenBank<sup>TM</sup> data base (accession number: AB045133). Since the peptide sequences of PHCR were also similar to the amino acid sequence of rabbit NDRD, a cDNA for PHCR was isolated by PCR-based homologue cloning. The characterization of the recombinant PHCR (rPHCR) and NDRD (rNDRD) shows that they are identical enzyme species which reduce alkyl phenyl ketones,  $\alpha$ -dicarbonyl compounds and retinals more efficiently than the known substrates of RaCR. Furthermore, we report the distribution of the enzymes in tissues of pig and rabbit as well as the subcellular localization of PHCR.

## 2. Methods

PHCR and RaCR were purified from hearts of castrated pigs and male Japanese white rabbits,

respectively, as described for the purification of the rabbit enzyme [16]. Protein sequence determination, including the reductive pyridylethylation of protein, its BrCN-cleavage, digestion by lysylendopeptidase, isolation of peptides and sequencing by automated Edman degradation, was performed as described previously [11,12].

The cDNA for rabbit NDRD was amplified from a total RNA preparation of the rabbit liver by reverse transcription (RT)-PCR using primers, racr1 and racr2. The racr1 corresponds to positions 1–17 of the cDNA, and racr2 is complementary to positions 767–783. The cDNA for PHCR was isolated from the total RNA sample of pig heart using a 3'-rapid amplification of cDNA ends (RACE) kit (Gibco-BRL) and primers, phcr1 and phcr2. The phcr1 (5'-ggcggcggggcagtta-3') and phcr2 (5'-tgttcccagacgtggaagt-3') were designed to anneal the sequences (positions from -52 to -37 and from -27 to -9, respectively) outside the putative open reading frame (ORF) of the pig expressed sequence tag (EST) sequences (accession numbers: AW359594 and AW359602) that are similar to the cDNAs for rabbit NDRD and human peroxisomal short-chain dehydrogenase (PSCD) [19]. The sequence of the cDNA was confirmed by repeating the cDNA isolation from the total RNA of the pig heart by RT-PCR, in which PCR was performed with *Pfu* DNA polymerase (Stratagene) and primers, phcr3 (5'-atggcagcaccgggggt-3' that corresponds to positions 1–17 of the cDNA) and phcr4 (5'-aaaccagttgataatgctg-3' that is complementary to positions 834–853).

Bacterial expression plasmids were prepared by inserting the cDNAs for rabbit NDRD and PHCR into pCR T7/CT TOPO vectors (Invitrogen) to express the enzymes without His-tag sequences. The constructs were transformed into *Escherichia coli* BL21(DE3)pLysS cells (Invitrogen), and the ORFs of the cDNAs in the expression plasmids were verified by nucleotide sequence analysis. Culture of the *E. coli* cells, induction of the recombinant enzymes and preparation of the cell extract were carried out as described previously [10,12]. rNDRD and rPHCR were purified from the cell extracts by essentially the same procedures for the purification of RaCR [16].



The reductase and dehydrogenase activities were determined by recording the change of absorbance at 340 nm of NADPH. The standard reaction mixture for CR activity consisted of 0.1 M potassium phosphate, pH 6.0, 0.1 mM NADPH, 1 mM 4-benzoylpyridine and enzyme in a total volume of 2.0 ml. The dehydrogenase activity was assayed with 0.25 mM NADP<sup>+</sup> and 0.1 M potassium phosphate buffer, pH 7.4, as the coenzyme and buffer, respectively. The activities for retinoids (Sigma) were measured as in Ref. [20], except that 0.1 mM NADPH and 0.1 M potassium phosphate, pH 7.4, containing 0.01% Tween 80 were used as the coenzyme and buffer, respectively. One unit of enzyme activity was defined as the enzyme amount that catalyzes the reduction or formation of 1  $\mu$ mol of NADPH or retinal per min at 25 °C.

The products of the all-*trans*-retinal reduction by the enzymes were analyzed by reverse-phase high performance liquid chromatography (RP-HPLC) [21]. The products of the enzymatic *n*-butyrophenone reduction were extracted into ethyl acetate and analyzed by normal-phase HPLC using a Daicel Chiralcel OJ-H 5  $\mu$ m column (4.6  $\times$  250 mm). When the column was eluted with *n*-hexane/2-propanol (95:5, v/v) at a rate of 0.5 ml/min, the retention times of authentic *S*-(-)-1-phenyl-1-butanol and its *R*-(+)-enantiomer were 33 and 35 min, respectively. The superoxide formation by redox cycling of quinone and its hydroquinone in the reduction of  $\alpha$ -dicarbonyl compounds by the enzyme was examined as described previously [6].

The frozen tissues ( $\approx$  1.0 g) of pig and rabbit were thawed and homogenized in 10 mM Tris-HCl, pH 7.5, containing 0.5 M NaCl to extract the basic PHCR and RaCR. The 105 000  $\times$  g supernatants of the homogenates were subjected to Western blot analysis using an anti-rPHCR antibody, which was raised in rabbits. The expression of mRNAs for PHCR and RaCR in the pig and rabbit tissues was analyzed by RT-PCR, in which PCR was performed using *Taq* DNA polymerase (Takara) and the primer pairs (phcr3 and phcr4 for PHCR cDNA, and racr1 and racr2 for RaCR cDNA).

To examine the localization of PHCR in mammalian cells, an additional expression plasmid was constructed. PHCR cDNA was amplified from the bacterial expression plasmid by PCR using primer combinations phcr5 and phcr6. The phcr5 (5'-ttgaattcggccaccatggccagcaccgggg-3') included an *EcoRI* site, and the phcr6 is V5 reverse primer (Invitrogen) that included a *SalI* site. The PCR product was subcloned at the *EcoRI* and *SalI* sites of a pGW1 vector, which is a kind gift from Dr Y. Nomoto (Gifu Pharmaceutical University). HeLa cells were transiently transfected with the pGW1/PHCR plasmids using a X-tremeGENE Q2 Transfection kit (Roche). Two days later, rPHCR expressed in the cells was stained with rabbit anti-rPHCR antibody and goat rhodamine-conjugated anti-rabbit IgGs (Chemicon International), and the red fluorescence in the cells was imaged using Zeiss LSM510 laser scanning confocal microscope. The distribution pattern of the expressed rPHCR in the cells was compared with that of an enhanced-green fluorescent protein fused with a C-terminal peroxisomal targeting signal (PTS1), SKL, (EGFP), which was co-expressed using pEGFP-Peroxi vectors (Clontech).

### 3. Results

#### 3.1. Protein sequencing and isolation of cDNA

PHCR was purified in a 7.1% yield (1.2 mg) from 200 g of pig heart. The subunit molecular weight of 27 kDa and substrate specificity for aromatic aldehydes and ketones were similar to those of RaCR that was isolated from rabbit heart (data not shown). To compare the structures between PHCR and RaCR, we initially determined sequences of the N-terminal 10-amino acids and three internal peptides of PHCR, and those of seven peptides derived from RaCR. The peptide sequences of RaCR completely matched the regions of the amino acid sequence deduced from a cDNA for rabbit NDRD, which shows 85% sequence identity with that for human PSCD [19] (Fig. 1). The sequences of the N-terminal region and peptides of PHCR were also similar to the deduced amino acid sequences of rabbit NDRD

```

PHCR  MASTGVERRKPLENKVALVTASTDGIGLAIARRLAQDGAHVVVSSRRKQENVDRTVATLQEGLSVTGTVC 70
NDRD  ---S---T---D---A---I-----I---Q---A---A---A-----
PSCD  ---S-MT---D---A-----F-----Q---QA-----

PHCR  HVGKAEDRRERLVAMAVNLHGGVDILVSNAAVNPFFGNLIDATEEVWDKILHVNVKATVLMTKAVVPEMEK 140
NDRD  -----T-L---I-----K-M-V-----DI---MA-----
PSCD  -----K---I-----S-M-V-----T-DI---PA-----

PHCR  RGGGSVLLIVSSVGAYHPFPNLGPYNVSKTALLGLTKNLAVELAPRNIRVNCLAPGLIKTNFSQVLWMDKA 210
NDRD  -----V---A-IA-FN--SG-----V-----L---AQ-----S--KA--E--
PSCD  -----V---IA-FS-S-GFS-----T--I-----S--RM-----E

PHCR  RKEYMKESLRIRRLGNPEDCAGIVSFLCSEDASYITGETVVVGGTASRL 260
NDRD  QE-NIIQK-----K--E-----A--AP---
PSCD  KE-S---T-----E-----P---

```

Fig. 1. Amino acid sequence alignment of PHCR with rabbit NDRD and human PSCD. Identical residues between PHCR and the other proteins are denoted by hyphens. The sequences determined by protein sequencing of the purified PHCR and RaCR are underlined in the deduced sequences of the respective animals. The residues in the coenzyme binding and active sites of the SDR family proteins are highlighted in bold. The accession numbers of the cDNAs for the enzymes: PHCR, AB062757; rabbit NDRD, AB045133; and PSCD, AF044127.

and human PSCD. Then, we searched pig EST sequences similar to the sequence of the cDNAs for rabbit NDRD and human PSCD in the EST database to isolate the cDNA for PHCR by PCR, and found the two EST sequences, showing 85% sequence identity with the region (positions from -67 to 210) of the human PSCD cDNA. A cDNA (853 bp) was isolated from the total RNA of pig heart by 3'-RACE using the primers, *phcr1* and *phcr2*, that were designed to anneal the putative non-coding regions of the two pig ESTs. The 783-bp ORF of the cDNA encoded a polypeptide of 260 amino acids with a molecular weight of 27.7 kDa and pI of 9.3. The partial sequences of PHCR perfectly matched the regions of the amino acid sequence deduced from the cDNA (Fig. 1), which indicates the authenticity of the cloned cDNA for PHCR. PHCR showed high amino acid sequence identity with rabbit NDRD (80%) and human PSCD (83%). As human PSCD has been reported to be a member of the SDR family [19], the several residues involved in the coenzyme binding and catalytic mechanism of this family proteins [5,22] are conserved in the sequences of both PHCR and rabbit NDRD. Since the properties of rabbit NDRD remain unknown, we isolated the cDNA for rabbit NDRD and investigated the enzymatic

activity with the recombinant enzyme as well as rPHCR.

### 3.2. Properties of rPHCR and rNDRD

The extracts of the *E. coli* cells transfected with the plasmids harboring the cDNAs for PHCR and rabbit NDRD exhibited NADPH-linked CR activities of 0.5 and 0.03 U/mg, respectively. The recombinant enzymes were each purified from 1 l of the cultured cells, and the respective yields (amounts) and specific activities of the final preparations were 32% (5.2 mg) and 24 U/mg for rPHCR; and 55% (4.4 mg) and 6.6 U/mg for rNDRD. SDS-PAGE of the two enzymes revealed a single 27-kDa protein band, and their gel exclusion chromatography on a Pharmacia Superdex 200 HR column resulted in a single peak with an apparent  $M_r$  of ~100 kDa, demonstrating tetrameric structures for the functional enzymes.

rPHCR and rNDRD reduced pyridine-4-aldehyde, 3- and 4-benzoylpyridines, menadione and 4-hexanoylpyridine that are substrates of RaCR [16], and the  $K_m$  values for the substrates (Table 1) are similar to those of RaCR [16] and PHCR (data not shown). The pH optima of the reductase activities of rPHCR and rNDRD were around

Table 1  
Kinetic constants for carbonyl compounds

| Substrate                                       | rNDRD |           |               | rPHCR |           |               |
|---|-------|-----------|---------------|-------|-----------|---------------|
|   | $K_m$ | $V_{max}$ | $V_{max}/K_m$ | $K_m$ | $V_{max}$ | $V_{max}/K_m$ |
| <i>Known substrates of RaCR</i>                 |       |           |               |       |           |               |
| Pyridine-4-aldehyde                             | 1.8   | 98.9      | 55            | 1.4   | 24.9      | 18            |
| 4-Benzoylpyridine                               | 0.69  | 13.3      | 19            | 0.29  | 30.2      | 104           |
| 3-Benzoylpyridine                               | 0.52  | 3.8       | 7             | 0.76  | 16.2      | 21            |
| Menadione                                       | 0.12  | 2.6       | 22            | 0.29  | 8.7       | 30            |
| 4-Hexanoylpyridine                              | 0.095 | 55.7      | 586           | 0.090 | 29.9      | 322           |
| <i>Alkyl phenyl ketones</i>                     |       |           |               |       |           |               |
| Nonanophenone                                   | 0.027 | 3.5       | 129           | 0.031 | 5.0       | 160           |
| Heptanophenone                                  | 0.063 | 6.5       | 103           | 0.028 | 6.3       | 223           |
| Hexanophenone                                   | 0.022 | 5.8       | 262           | 0.021 | 10.2      | 458           |
| Valerophenone                                   | 0.11  | 5.8       | 52            | 0.052 | 9.3       | 178           |
| <i>n</i> -Butyrophenone                         | 0.18  | 3.3       | 19            | 0.17  | 11.6      | 68            |
| Propiophenone                                   | 0.89  | 1.0       | 1             | 0.89  | 3.0       | 3             |
| <i><math>\alpha</math>-Dicarbonyl compounds</i> |       |           |               |       |           |               |
| Diacetyl  | 13    | 110       | 8             | 4.5   | 28.8      | 6             |
| 2,3-Hexanedione                                 | 1.7   | 115       | 68            | 0.47  | 22.6      | 48            |
| 1-Phenyl-1,2-propanedione                       | 0.40  | 115       | 287           | 0.04  | 43.5      | 1090          |
| Benzil  | 0.11  | 66.8      | 607           | 0.13  | 36.5      | 281           |
| Isatin  | 0.11  | 83.6      | 760           | 0.030 | 36.5      | 1220          |
| 1-Phenylisatin                                  | 0.006 | 152       | 25 300        | 0.004 | 39.2      | 9800          |
| 16-Ketoestrone                                  | 0.028 | 48.7      | 1739          | 0.086 | 23.3      | 270           |
| 9,10-Phenanthrenequinone                        | 0.001 | 121       | 121 000       | 0.002 | 39.2      | 19 600        |

The  $K_m$  (mM),  $V_{max}$  (U/mg) and  $V_{max}/K_m$  (U/mg/mM) values were determined at pH 6.0.

pH 5.5 and 6.0, respectively. The two enzymes were inhibited by kaemferol, quercetin, genistein and myristic acid, and the respective  $IC_{50}$  (concentrations required for 50% inhibition) values were 15, 16, 28 and 25  $\mu$ M for rPHCR, and were 4.0, 5.2, 10 and 5.8  $\mu$ M for rNDRD. The properties of rNDRD were essentially identical to those reported for RaCR [16,23,24], which further supports the identity of the two enzymes.

rNDRD and rPHCR did not reduce aliphatic aldehydes and ketones (acetaldehyde, *n*-butyraldehyde and 2-butanone), sugars (D-glucuronate, D/L-xylulose, D/L-xylose, D/L-glucose and 3-deoxyglucosone), 3/20-ketosteroids, prostaglandins ( $A_1$ ,  $E_2$ , and  $D_2$ ) and sepiapterine. However, they exhibited high reductase activity for alkyl phenyl ketones and  $\alpha$ -dicarbonyl compounds with aromatic ring(s) (Table 1). Among the substrates, 9,10-phenanthrenequinone was the best substrate showing an extremely high  $V_{max}/K_m$  value. It should be noted that the superoxide formation was observed

in the reduction of 9,10-phenanthrenequinone, but not in the reduction of the other  $\alpha$ -dicarbonyl compounds. Since NDRD was identical to RaCR, we also tested retinoids as the substrates of the recombinant enzymes at pH 7.4. The enzymes reduced all-*trans*-retinal and 9-*cis*-retinal, and the  $K_m$  and  $V_{max}/K_m$  values for all-*trans*-retinal were comparable to those of endogenous  $\alpha$ -dicarbonyl compounds, isatin and 16-ketoestrone, determined under the same conditions (Table 2). When the time-dependent reduction of all-*trans*-retinal was analyzed by RP-HPLC, all-*trans*-retinol (retention time = 10.0 min) increased with a decrease of all-*trans*-retinal (retention time = 12.4 min) upon the incubation time, and NADPH oxidation, all-*trans*-retinal reduction and all-*trans*-retinol formation were almost in a ratio of 1:1:1. In the reverse reaction with  $NADP^+$  as the coenzyme, the enzymes oxidized all-*trans*-retinol, although the  $V_{max}/K_m$  value was much lower than those for the retinals. In addition, the enzymes oxidized *S*-

Table 2  
Kinetic constants for substrates in the reduction and dehydrogenation by rNDRD and rPHCR

| Substrate                        | rNDRD |                   |               | rPHCR |           |               |
|----------------------------------|-------|-------------------|---------------|-------|-----------|---------------|
|                                  | $K_m$ | $V_{max}$         | $V_{max}/K_m$ | $K_m$ | $V_{max}$ | $V_{max}/K_m$ |
| <i>Reduction</i>                 |       |                   |               |       |           |               |
| All- <i>trans</i> -Retinal       | 0.007 | 2.54              | 363           | 0.003 | 1.7       | 618           |
| 9- <i>cis</i> -Retinal           | 0.079 | 6.34              | 80            | 0.032 | 2.8       | 87            |
| Isatin                           | 0.061 | 34.5              | 566           | 0.005 | 4.5       | 900           |
| 16-Ketoestrone                   | 0.045 | 24.2              | 538           | 0.017 | 3.7       | 218           |
| 9,10-Phenathrenequinone          | 0.001 | 78.0              | 78 000        | 0.001 | 3.9       | 3900          |
| <i>Dehydrogenation</i>           |       |                   |               |       |           |               |
| All- <i>trans</i> -Retinol       | 0.034 | 0.05              | 1.4           | 0.029 | 0.04      | 1.5           |
| <i>S</i> -(-)-1-Phenyl-1-butanol | 0.27  | 1.35              | 5.0           | 0.35  | 3.3       | 9.5           |
| <i>R</i> -(+)-1-Phenyl-1-butanol | –     | n.s. <sup>a</sup> | –             | 1.2   | 0.13      | 0.1           |

The  $K_m$  (mM),  $V_{max}$  (U/mg) and  $V_{max}/K_m$  (U/mg/mM) values were determined at pH 7.4.

<sup>a</sup> No significant activity was detected at substrate concentration of 4 mM.

(-)-1-phenyl-1-butanol in preference to its *R*-(+)-enantiomer, and showed broad pH dependency from 7.0 to 10.0. The stereo selectivity in the oxidation by the enzymes was coincident with that of the reduction of *n*-butyrophenone, in which only *S*-(-)-1-phenyl-1-butanol was formed as the product. rPHCR and rNDRD showed absolute coenzyme specificity for NADP(H), and the respective  $K_m$  values for NADPH were 2 and 4  $\mu$ M.

### 3.3. Tissue distribution

The tissue distribution of the mRNAs for PHCR and RaCR was initially assessed by RT-PCR. As illustrated in Fig. 2a, we detected the expression of the tetrameric CR transcript in various tissues of pig and rabbit, although the expression levels in tissues seemed to be different depending on the two species. The anti-rPHCR antibody weakly cross-reacted with rRaCR on Western blot analysis (Fig. 2b), and more than 70% of CR activity was recovered in 105 000  $\times$  *g* supernatants of the homogenates when the tissues were homogenized in the buffer containing 0.5 M NaCl. Therefore, the expression levels of PHCR and RaCR in the 0.5 M NaCl extracts of the tissues were examined by Western blot analysis using the antibody and by measuring CR activity (Fig. 2c). The tissue distribution patterns of the

enzyme proteins and activities almost perfectly correlated with the results by RT-PCR.

The purification of soluble PHCR and RaCR from the tissues and high recovery of the enzyme activity in the 105 000  $\times$  *g* supernatants of the tissue homogenates suggested that the enzymes are cytosolic. However, the PTS1-like sequence, SRL [25], was conserved in the sequences of PHCR and rabbit NDRD, i.e. RaCR (Fig. 1). To elucidate the subcellular localization of the enzymes, HeLa cells were transfected with the vectors harboring the cDNAs for PHCR and the peroxisome-labeling protein, EGFP. The distribution pattern of rPHCR in the cells was superimposable on that of EGFP (data not shown), which indicates that PHCR is a peroxisomal enzyme.

## 4. Discussion

The cloning and expression of a cDNA encoding the functional subunit of tetrameric PHCR indicates that the enzyme belongs to the SDR family and exhibits broad substrate specificity for aromatic aldehydes, quinones, alkyl phenyl ketones,  $\alpha$ -dicarbonyl compounds and retinals. PHCR shows low sequence identity (<24%) with other mammalian monomeric and tetrameric CRs [2–4,11–13], but shares high sequence identity with human PSCD [19] and rabbit NDRD,